

Probing Double-Charged Higgs Boson Production in HERA Experiments

Mr.M.Uppa Mahesh

Assistant Professor, Department of H&S,
Malla Reddy College of Engineering for Women.,
Maisammaguda., Medchal., TS, India

Article Info

Received: 26-01-2023

Revised: 12-02-2023

Accepted: 24-02-2023

Abstract:

In ep collisions, a search for the sole synthesis of doubly charged Higgs bosons H is provided. The Higgs decays into a high mass pair of leptons with the same charge, one of which is an electron, are used to look for the signal. Up to 118 pb-1 of ep data from the H1 experiment at HERA are used in the analysis. No evidence of doubly-charged Higgs production is shown, and upper limits on the Yukawa couplings of the Higgs boson to an electron-lepton pair are derived based on mass. A lower limit of 141 GeV on the H mass is found at the 95% confidence level under the assumption that the doubly-charged Higgs only decays into an electron and a muon via an electromagnetic coupling of strength $h_e = 4m_e$ 0.3. For

Introduction

Doubly-charged Higgs bosons ($H^{\pm\pm}$) appear when the Higgs sector of the Standard Model (SM) is extended by one or more triplet(s) with non-zero hypercharge [1–3]. Examples are provided by some left-right symmetric models [4], or their supersymmetric extensions, which are of particular interest since they provide a mechanism to generate small non-zero neutrino masses. Such models can lead to a doubly-charged Higgs boson light enough [5] to be produced at the existing colliders. The Higgs triplet(s) may be coupled to matter fields via Yukawa couplings which are generally not related to the fermion masses. A non-vanishing coupling of a doubly-charged Higgs to an electron would allow its single production in ep collisions at HERA. This possibility is investigated in this Letter with a search for doubly-charged Higgs bosons decaying into a high mass pair of same charge leptons, one of them being an electron. An analysis of multi-electron events was already presented by the H1 Collaboration [6]. Six events were observed with a di-electron mass above 100 GeV, a domain in which

the Standard Model prediction is low. In the present Letter the compatibility of these events with the hypothesis of a doublycharged Higgs coupling to $e\bar{e}$ is addressed and a further search for a $H^{\pm\pm}$ boson coupling to $e\bar{e}$ and $e\bar{e}$ is performed. The analysis is based on ep data collected by the H1 experiment between 1994 and

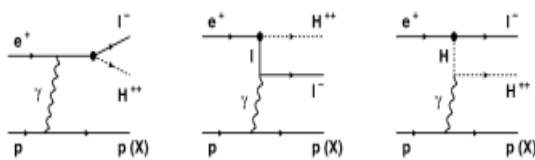
2000, which amount to a luminosity of up to 118 pb-1.

Phenomenology

At tree level, doubly-charged Higgs bosons couple only to charged leptons and to other Higgs and gauge bosons. Couplings to quark pairs are forbidden by charge conservation. The couplings of a doubly-charged Higgs to charged leptons can be generically described by the Lagrange

$$\mathcal{L} = \sum_{i,j} h_{i|l_j}^{L,R} H_{L,R}^{++} \bar{l}_i^c P_{L,R} l_j + \text{h.c.}, \quad (1)$$

where l are the charged lepton fields, l^c denote the charge conjugate fields, i, j are generation indices, and $P_L, R = (1 \mp \gamma_5)/2$. The Higgs fields H^{++} L, R coupling to left- or right-handed leptons correspond to different particles and not all models predict their simultaneous existence. The Yukawa couplings $h_{i|l_j}^{L,R}$ are free parameters of the model. The phenomenology of doubly-charged Higgs production at HERA was first discussed in [7]. For a non-vanishing coupling $h_{i|l_j}^{L,R}$, the single production of a doubly-charged Higgs boson is possible at HERA in e^+e^- interactions via the diagrams shown in Fig. 1, where a photon is radiated off the proton or one of its constituent quarks. The proton may remain intact or be broken



case, where the initial proton remains intact (dissociates). The contribution of Z exchange can be safely neglected.

during this interaction, leading to an elastic or inelastic reaction, respectively. With longitudinally unpolarised lepton beams, as were delivered by HERA until 2000, the $H^{\pm\pm}$ production cross section does not depend on whether the Higgs couples to left- or right-handed leptons. Hence a generic case is considered here of a doubly-charged Higgs boson which couples to either left or right-handed leptons and the L, R indices are dropped in the following. Within the mass range considered in this analysis, it is assumed that decays of the $H^{\pm\pm}$ into gauge bosons and other Higgs particles are not allowed kinematically such that the doubly-charged Higgs only decays via its Yukawa couplings into a lepton pair. Indirect upper bounds on the Yukawa couplings of a doublycharged Higgs to leptons are reviewed in [8]. The coupling h_e of a doubly-charged Higgs to an electron pair is constrained by the contribution of virtual $H^{\pm\pm}$ exchange to Bhabha scattering in e^-e^- collisions. A recent OPAL analysis [9] sets the constraint $h_e < 0.14$ for a doubly-charged Higgs mass $M_H = 100$ GeV. From low energy e^-e^- data, coupling values of 0 (0.1) are allowed for h_e and h_{τ} for a Higgs mass of 100 GeV [10]. Taking these indirect constraints into account, the production of a doubly-charged Higgs mediated by h_e , h_{τ} or $h_{\tau\tau}$ might be observable at HERA. The Higgs signal would manifest itself as a peak in the invariant mass distribution of same charge e^-e^- , e^-e^+ or e^+e^+ leptons, respectively. For the range of masses and couplings probed in this analysis, the Higgs decay length is vanishingly small but its width remains negligible compared to the experimental resolution on the mass of the lepton pair

Simulation of the signal and Standard Model backgrounds

The calculation of the cross section for doubly-charged Higgs production, as well as the simulation of signal events, relies on a dedicated Monte Carlo program developed for this analysis. The differential cross sections are integrated using the VEGAS package [11]. Different approaches are followed depending on the photon virtuality Q^2 and on the mass W of the hadronic final state: • In the inelastic region ($W > M_P + m_{\pi}$, with the proton mass M_P and the pion mass m_{π}) and when the

Fig. 1. Diagrams for the single production of a doubly-charged Higgs boson in e^-p collisions at HERA via the hell coupling. The hadronic final state is denoted by p (X) in the elastic (inelastic)

photon virtuality is large ($Q^2 > 4$ GeV 2), the interaction involves a quark inside the proton. The squared amplitude of the process $q_i \rightarrow \text{echo} \pm q$ is evaluated using the Compel package [12,13]. The parton densities in the proton are taken from the CTEQ4L [14] parameterisation and are evaluated at the scale Q^2 . The parton shower approach [15] based on the DGLAP [16] evolution equations is applied to simulate QCD corrections in the initial and final states, and the hadronization is performed using PYTHIA 6.1 [15]. • For the elastic region ($W = M_P$) and the inelastic region at low Q^2 ($W > M_P + m_{\pi}$, $Q^2 < 4$ GeV 2), the squared amplitude is calculated using the FORM program [17]. The hadronic tensor is parameterised in terms of the usual Elec

paramagnetic structure functions $F_1(x, Q^2)$ and $F_2(x, Q^2)$ of the proton, where $x = Q^2 / (W^2 + Q^2 - m^2 p)$. For the elastic process these structure functions are expressed in terms of the electric and magnetic form factors of the proton. For the low Q^2 inelastic region they are taken from analytical parameterisations [18]. The simulation of the hadronic final state for low Q^2 inelastic events is performed via an interface to the SOPHIA program [19]. For a Yukawa coupling h_e or h_{τ} of electromagnetic strength ($h = 4\pi \alpha_{em} (Q^2 = 0)$)

0.3) the total cross section amounts to 0.39 pb (0.04 pb) for a Higgs mass of 100 GeV (150 GeV). The low Q^2 (high Q^2) inelastic contribution is found to be $\sim 30\%$ ($\sim 20\%$) of the total cross section in the mass range 80–150 GeV. The cross section for producing a doublycharged Higgs via a coupling h_e is lower by about 40% due to the non-negligible mass of the τ lepton produced in association with the Higgs. The theoretical uncertainty on the cross sections obtained is taken to be 4% in the mass range considered. This is derived from an assessed uncertainty of 2% on the proton form factors [20] and from the uncertainty on the scale at which the parton densities for the inelastic contribution are evaluated. The lateTer uncertainty is estimated from the variation of the computed cross section as this scale is changed from $Q^2/2$ to $2Q^2$.

Separate signal event samples corresponding to the production and decay of a doubly-charged Higgs via a coupling h_e , h_{τ} and $h_{\tau\tau}$ have been produced for Higgs masses ranging between 80 and 150

GeV, in steps of 10 GeV. Di-electron production, which proceeds mainly via twophoton interactions, constitutes an irreducible background for eye final states. The production of muon or tau pairs costtotes a background for the eel and eel analyses when the scattreed electron is detected. The Cabibbo–Parisi process eye $\rightarrow \gamma, Z \rightarrow \text{all}$, in which the incoming electron interacts with an ElecTron emitted from a photon radiated from the proton, contributes at high transverse momentum only. The Drell–Yan process was calculated in [21] and found to be negligible. All these processes are simulated using the GRAPE Monte Carlo generator [22], which also takes into account contributions from Bremsstrahlung with subsequent photon conversion into a lapton pair and electroweak contributions. Experimental backgrounds come dominantly from neutral current deep inelastic scattering (NC DIS) where a jet is misidentified as an electron, a muon or a tau. Compton scattering is also a source of background for eye final states when the photon is misidentified as an electron. These processes are simulated with the DJANGO [23] and WABGEN [24] generators. All generated events are passed through the full simulation of the H1 apparatus and are reconstructed using the same program chain as for the date

The H1 detect

A detailed description of the H1 experiment can be found in [25]. Only the H1 detector components relevant to the present 436 H1 Collaboration / Physics Letters B 638 (2006) 432–440 analysis are briefly described here. Jets and electrons are measured with the liquid argon (Larr) calorimeter [26], which covers the polar angle range $4^\circ < \theta < 154^\circ$. Electromagnetic shower energies are measured with a precision of $\sigma(E)/E = 12\%/\sqrt{E/\text{GeV}} \oplus 1\%$ and hadronic energies with $\sigma(E)/E = 50\%/\sqrt{E/\text{GeV}} \oplus 2\%$, as determined in test beams [27]. In the backward region a lead/scintillating-fibre (Spa Cal) calorimeter [28] covers the range $155^\circ < \theta < 178^\circ$. The central ($20^\circ < \theta < 160^\circ$) and forward ($7^\circ < \theta < 25^\circ$) tracking detectors are used to measure charged particle trajectories, to reconstruct the interaction vertex and to supplement the measurement of the hadronic energy. The Larr and inner tracking detectors are enclosed in a super-conducting magnetic coil with a strength of 1.15 T. The return yoke of the coil is the outermost part of the detector and is equipped with streamer tubes forming the cantral muon detector ($4^\circ < \theta < 171^\circ$). In the forward region of the detector ($3^\circ < \theta < 17^\circ$) a set of drift chamber layers (the forward muon system) detects muons and, together with an iron toroidal magnet, allows a momentum measurement. The lugminosity measurement is based on the Bethe–Heitler process $e\gamma \rightarrow \text{up}$, where the photon is detected in a

calorimeter locited downstream of the interaction point.

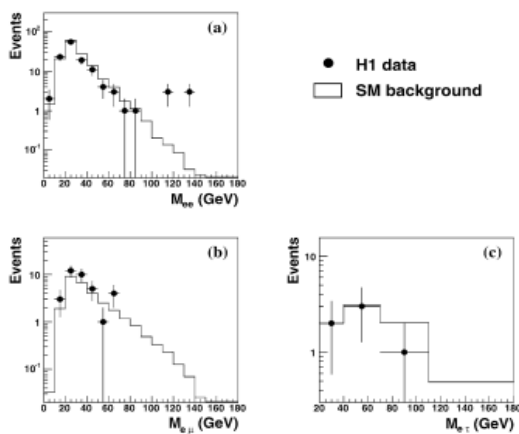
Data analysis:

The analyses of eye and eel final states use the full esp. data set recorded in the period 1994–2000, which corresponds to an integrated luminosity of 118 pb $^{-1}$. The analysis of eel finil states makes use of the esp. data collected in the years 1996–1997 and 1999–2000, which amount to a luminosity of 88 pb $^{-1}$. The HERA collider was operated at a centre-of-mass energy \sqrt{s} of 300 GeV in 1994–1997 and of 318 GeV in 1998–2000. Events are first selected by requiring that the longitudinal position of the vertex be within 35 cm around the nominal inraction point. In addition, topological filters and timing vetoes are applied to remove background events induced by cosmic showers and other non-ep sources. The main triggers for the events are provided by the Larr calorimeter and the muon systeem

Lepton identification

An electron candidate is identified by the presence of a compact and isolated electromagnetic energy deposit above 5 GeV in the Larr or Spa Cal calorimeter. The energy of the electron candidate is measured from the calorimetric Informaton. In the angular range $20^\circ < \theta < 150^\circ$ the electron identdeification is complemented by tracking conditions; in which case the direction of the electron candidate is given by that of the associated track. Electron candidates in the forward region, $5^\circ < \theta < 20^\circ$, are required to have an energy above 10 GeV. A muon candidate is identified by associating an isolated track in the forward muon system or in the inner tracking system with a track segment or an energy deposit in the instructmited iron. The muon momentum is measured from the track curvature in the toroidal or solenoidal magnetic field, respecttively. Tau leptons are preselected as described in [29] by requireIng a track with transverse momentum above 5 GeV measured in the inner tracking detector. The leptonic tau decays $\tau \rightarrow e\bar{v}v$ and $\tau \rightarrow \mu\bar{v}v$ are reconstructed by matching the selected track to an identified electron or muon. Tracks that are not identified as electrons or muons are attributed to hadronic tau decays if at least 40% of the track momentum is reconstructed in the Larr calorimeter as matched clustered energy. In that case it is moreover required that the track belong to a narrow jet: No other track should be reconstructed within $0.15 < R < 1.5$ around the track direction, where $R = \sqrt{\eta^2 + \phi^2}$ with η and ϕ being the distances in pseudo rapidity and azimuthal angle, resporthively. The transverse momentum and the direction of the τ candidate are approximated by those of the associated track.

This analysis is based on the published H1 measurement of multi-electron production [6]. The event selection requires at least two central ($20^\circ < \theta_e < 150^\circ$) electron candidates, one of them with a transverse momentum $P_{e1} T > 10$ GeV (ensuring a trigger efficiency close to 100% [30]) and the other one with $P_{e2} T > 5$ GeV. After this preselection, 125 events are observed, in good agreement with the SM expectation of 137.4 ± 10.7 . In each event, the two highest PT electrons, one of those being possibly outside the central region, are assigned to the Higgs candidate. The distribution of their invariant mass M_{ee} is shown in Fig. 2(a). At low mass a good agreement is observed between data and the SM expectation which is largely dominated by $\gamma\gamma$ contributions. Six events are observed at $M_{ee} > 100$ GeV, compared to the SM expectation of 0.53 ± 0.08 . Further selection criteria are then applied, which are designed to maximise the sensitivity of the analysis to a possible H $\pm\pm$ signal. The charge measurement of the two leptons assigned to the Higgs candidate is exploited. In esp. (e-p) collisions, where H $++$ (H $--$) bosons could be produced, events in which one of the two leptons is reliably assigned a negative (positive) charge are rejected. The charge assignment requires that the curvature κ of the track associated with the lepton be measured with an error $\delta\kappa$ satisfying $|\kappa/\delta\kappa| > 2$. The precise calorimetric measurement of the electron transverse momenta is further exploited by applying an additional M_{ee} dependent cut on the sum of the transverse momenta of the two electrons assigned to the Higgs candidate. The lower bound is optimised to keep 95% of the signal and varies between 45 and 120 GeV. This cut reduces the background by typically 50%, suppressing $\gamma\gamma$ events in which a large mass is reconstructed from low PT electrons, as occurs when a forward electron is combined, we



the scattered electron detected at a large angle. The efficiency for selecting signal events varies from 50% for a H $\pm\pm$ mass of 80 GeV to 35% for a H $\pm\pm$ mass of 150 GeV. In this mass range the resolution on M_{ee} varies between 2.5 and 5 GeV. After these

requirements, 3 events are observed at $M_{ee} > 65$ GeV, in agreement with the SM expectation of 2.45 ± 0.11 events. Amongst the six events 15 at $M_{ee} > 100$ GeV, only one satisfies the final selection criteria

Analysis of the $H \rightarrow eel$ decay

Events having one electron and one muon with minimal transverse momenta of $P_e T > 10$ GeV and $P_\mu T > 5$ GeV are selected. The polar angle of electron candidates is restricted to $20^\circ < \theta_e < 140^\circ$ to reduce the large background arising from NC DIS events. The θ range for muon candidates extends towards low angles, $10^\circ < \theta_\mu < 140^\circ$, which increases the efficiency for high H $\pm\pm$ masses. The minimum transverse momentum required for electron candidates ensures a trigger efficiency close to 100% for these events. After this preselection, 35 data events are observed compared to a SM expectation of 29.6 ± 3.4 . In each event, the highest PT electron and muon which fulfil the above angular cuts are assigned to the Higgs candidate and the distribution of their invariant mass $M_{e\mu}$ is shown in Fig. 2(b). A good agreement is observed between the data and the SM expectation, which is dominated by $\gamma\gamma$ contributions. For the final selection of $H \rightarrow eel$ candidates the charge of the e and μ is exploited using the same criteria as used in Sec

ton 5.2. The efficiency for selecting signal events varies from 55% to 40% for a H $\pm\pm$ mass between 80 and 150 GeV. The resolution on $M_{e\mu}$ varies between 3 and 8 GeV. For $M_{e\mu} > 65$ GeV one event is observed while 4.17 ± 0.44 events are expected from the SM.

The search for a H $++$ boson decaying into eel is performed in three final states, depending on whether the τ decays into an electron, a muon or hadronically (h). Details of this analysis can be found in [29]. Events are selected which contain either two electrons (ee), or an electron and a muon (eel), or an ElecTron and a hadronic τ candidate (eh) as defined in Section 5.1. The two leptons, or the electron and the hadronic- τ candidate, should have a transverse momentum above 5 GeV and be in the angular range $20^\circ < \theta < 140^\circ$. If more than one electron, muon or hadronic τ candidate fulfils these requirements, the one with the highest PT is assigned to the Higgs candidate. The two particles assigned to the Higgs should be separated from each other by $R > 2.5$ in pseudo rapidity-azimuth. One of them must have a transverse momentum above 10 GeV, which ensures a trigger efficiency above 95% in all three classes. For events in the eel class the polar angle of the electron candidate is required to be below 120° . A significant amount of missing transverse

and longitudinal momentum is expected due to the neutrinos produced in the τ decays.

Events in the eye class are required to have a missing transverse momentum $P_{miss} T > 8$ GeV. For the eh class, which suffers from a large NC DIS background, it is required that $P_{miss} T > 11$ GeV, that the energy deposited in the Spa Cal calorimeter be below 5 GeV, and that the variable $-I_{Eid} - \sum_i p_i z_i$, where the sum runs over all visible particles, be smaller than 49 GeV. For fully contained events

$I_{Eid} - \sum_i p_i z_i$ is expected to peak at twice the lepton beam energy $E_0 = 27.5$ GeV, i.e., 55 GeV, while signal events are concentrated at lower values due to the non-observed neutrinos. In total 6 events are preselected, in agreement with the SM prediction of 7.8 ± 1.5 . In each class, the eel invariant mass M_{ee} is reconstructed by imposing longitudinal momentum and energy conservation, and by minimising the total momentum imbalance in the transverse plane. Tau leptons are assumed to decay with a vanishing opening angle. This method yields a resolution of about 4 GeV on the mass M_{ee} . Fig. 2(c) shows the eel invariant mass distribution of the selected events together with the SM expectation. For the final selection, events are rejected if the track associated with one of the Higgs decay product candidates is reliably assigned a negative charge, opposite to that of the incoming lepton beam. The signal efficiencies depend only weakly on M_H . The fractions of simulated $H \rightarrow eel$ events which are reconstructed in the various classes are given in Table 1, for an example mass of $M_H = 100$ GeV. The total efficiency on the signal amounts to about 25%. The final event yields are also shown in Table 1. Only one event (in the eh class) satisfies the final criteria, while 2.1 ± 0.5 events are expected.

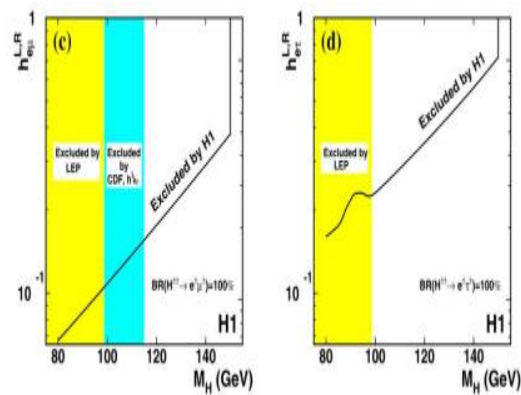
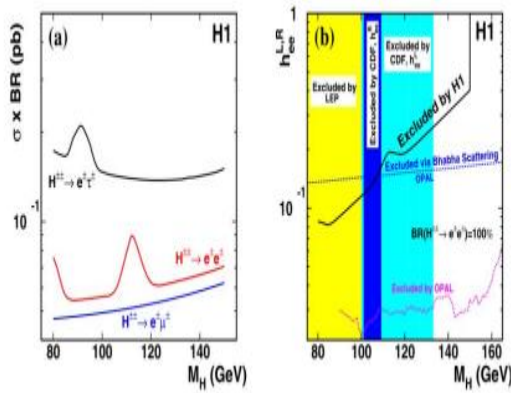


Fig. 3. (a) Upper limits at the 95% confidence level on the $H \pm$ production cross section times the branching ratio for the $H \pm$ to decay into eye, eel or ee, as a function of the Higgs mass. (b)–(d) Upper limits on the coupling hell assuming that the $H \pm$ couples only (b) to eye, (c) to ee or (d) to ee. Regions above the curves are excluded. The constraints obtained from pair production at LEP and at CDF and from single production at OPAL are also shown.

Systematic uncertainties

The systematic uncertainties attributed to the Monte Carlo predictions for the eye analysis are detailed in [6]. The dominant systematic uncertainty is due to the electron-track association efficiency, which is 90% on average with an uncertainty increasing with decreasing polar angle from 3% to 15%. Systematic errors due to the uncertainty on the electromagnetic energy scale (known at the 0.7% to 3% level in the central and forward regions of the Larr calorimeter, respectively) and on the trigger efficiency (3%) are also taken into account. For the eel analysis, the dominant additional systematic uncertainty is due to the muon identification efficiency known within 6% [31]. The uncertainty due to the reconstruction efficiency of the central tracking detector for central muons con

tributes an additional 3%. The muon momentum scale is known within 5%, and the trigger efficiency for eel final states is known within 3%. The same systematic uncertainties affect the SM expectations in the eye and eel classes of the eel analysis. The uncertainty of the hadronic energy scale in the Larr calorimeter (4%) constitutes another source of uncertainty due to the cuts applied on the $P_{miss} T$ and

$I_{Eid} - \sum_i p_i z_i$ variables. For the eh event class the dominant uncertainties on the SM expectation, coming mainly from NC DIS processes, are due to the uncertainty of 3% of the track efficiency, to that of the hadronic energy scale, and to that (15%) of the hadronization model. The luminosity measurement leads to a normalisation uncertainty of

1.5%. For both the expected signal and the predicted background, the systematic uncertainties resulting from the sources listed above are added in quadrature.

Interpretation

With the final Higgs selection, no significant excess over the SM expectation is observed. Upper limits on the $H^{\pm\pm}$ production cross section times the branching ratio for the $H^{\pm\pm}$ to decay into one of the analysed final states are derived as a function of the $H^{\pm\pm}$ mass and are shown in Fig. 3(a). The limits are presented at the 95% confidence level and are obtained using a modified frequentist approach [32]. Statistical uncertainties, as

well as the influence of the various systematic uncertainties on both the shape and the normalisation of the mass distributions for signal and background events, are taken into account. The best sensitivity is obtained for a $H^{\pm\pm}$ produced and decaying via $h\bar{e}$, with upper limits around 0.05 pb. Assuming that only one Yukawa coupling $h\bar{e}$ is nonvanishingly small, these constraints are translated into mass dependent upper limits on the coupling $h\bar{e}$, as shown in Fig. 3(b)–(d). If the doubly-charged Higgs boson couples only to an ElecTron pair (Fig. 3(b)) the eye analysis rules out $H^{\pm\pm}$ masses below 138 GeV for a coupling $h\bar{e}$ of the electromagnetic strength, $h\bar{e}$ _____

0.3. The result is compared to the bounds obtained from searches for $H^{\pm\pm}$ pair production at LEP [33] and by the CDF experiment [34], and to both the indirect and direct limits obtained by the OPAL experiment [9], the latter being the most stringent. The OPAL experiment has also set similar stringent constraints on the independently of the Higgs decay mode. These constraints also exclude a sizeable $H^{\pm\pm}$ production at HERA via $h\bar{e}$ followed by the $H^{\pm\pm}$ decay via $h\mu\mu$ or $h\tau\tau$, which is consistent with the non-observation of a resonance signal in the $\mu\mu$ [31] and $\tau\tau$ [29] final states in the present H1 data. Assuming that the doubly-charged Higgs boson couples only to an electron–muon (electron–tau) pair, the ee (ee) analysis allows masses below 141 GeV (112 GeV) to be ruled out for the _____

0.3 (he) _____ 0.3, as shown in Fig. 3(c) (Fig. 3(d)). The H1 limits extend the excluded region in the electron–muon and electron–tau channels to masses that are beyond those reached in previous searches for pair production at LEP [33] and the Tevatron [34].

Conclusion

A search for the single production of doubly-charged Higgs bosons coupling to ee, ee or ee is presented. In a previous model independent multi-electron analysis, H1 observed six events with a di-electron mass above 100 GeV, a region where the

Standard Model expectation is small. Out of the six events, only one is compatible with the signature of a doubly-charged Higgs boson. No electron–muon or electron–tau event is found in this mass domain. This analysis places new limits on the $H^{\pm\pm}$ mass and its Yukawa couplings $h\bar{e}$ to an electron–lepton pair. Assuming that the doubly-charged Higgs boson only couples to electron–muon (electron–tau) pairs, a limit of 141 GeV (112 GeV) is obtained on the Higgs mass, for a coupling $h\bar{e}$ _____ 0.3 (he) _____ 0.3) corresponding to an interaction of electromagnetic strength

Acknowledgements

We are grateful to the HERA machine group whose outstanding efforts have made this experiment possible. We thank the engineers and technicians for their work in constructing and maintaining the H1 detector, our funding agencies for financial support, the DESY technical staff for continual assistance and the DESY directorate for support and for the hospitality which they extend to the non-DESY members of the collaboration. We are especially grateful to J. Malampaya and N. Romanenko for providing the doubly-charged Higgs LaGrange implementation in Compel which was used in this analysis. We would also like to thank K. Hutz and E. Boos for their help and valuable discussions.

References

- [1] G.B. Gemini, M. Roncelli, Phys. Lett. B 99 (1981) 411.
- [2] J.C. Pati, A. Salam, Phys. Rev. D 10 (1974) 275; R.E. Marshak, R.N. Mohapatra, Phys. Lett. B 91 (1980) 222.
- [3] R.N. Mohapatra, G. Nanovic, Phys. Rev. Lett. 44 (1980) 912.
- [4] G. Nanovic, R.N. Mohapatra, Phys. Rev. D 12 (1975) 1502; R.N. Mohapatra, R.E. Marshak, Phys. Rev. Lett. 44 (1980) 1316; R.N. Mohapatra, R.E. Marshak, Phys. Rev. Lett. 44 (1980) 1643, Erratum. [5] C.S. Aulakh, A. Melo, G. Nanovic, Phys. Rev. D 57 (1998) 4174, hep-ph/9707256; Z. Chacko, R.N. Mohapatra, Phys. Rev. D 58 (1998) 015003, hep-ph/9712359; B. Dutta, R.N. Mohapatra, Phys. Rev. D 59 (1999) 015018, hep-ph/9804277.
- [6] A. Katas, et al., H1 Collaboration, Eur. Phys. J. C 31 (2003) 17, hep-ex/0307015. [7] E. Accomando, S. Petrarca, Phys. Lett. B 323 (1994) 212, hep-ph/9401242.
- [8] M.L. Swartz, Phys. Rev. D 40 (1989) 1521; J.F. Gunion, et al., Phys. Rev. D 40 (1989) 1546; M.

Losingly, S. Petrarca, Phys. Lett. B 226 (1989) 397; G. Barenboim, K. Hutu, J. Malampaya, M. Radial, Phys. Lett. B 394 (1997) 132, hep-ph./9611362; S. Godfrey, P. Kalnik, N. Romanenko, Phys. Rev. D 65 (2002) 033009, hep-ph./0108258.

[9] G. Abbie Ndi, et al., OPAL Collaboration, Phys. Lett. B 577 (2003) 93, hep-ex/0308052. [10] F. Cuypers, S. Davidson, Eur. Phys. J. C 2 (1998) 503.

[11] G.P. Lepage, An adaptative multidimensional integration program, CLNS80/447, 1980. [12] E. Boos, et al., Compel Collaboration, Null. In strum. Methods A 534 (2004) 250, hep-ph./0403113; A. Puhoi, et al., hep-ph./9908288, available at <http://theory.sinp.msu.ru/compel>.

[13] S. Godfrey, P. Kalnik, N. Romanenko, Phys. Rev. D 65 (2002) 033009, hep-ph./0108258.

[14] H.L. Lai, et al., Phys. Rev. D 55 (1997) 1280, hep-ph./9606399.

[15] T. Sjostrom, et al., Compute. Phys. Common. 135 (2001) 238, hepph./0010017.

[16] V.N. Gribov, L.N. Lipitor, Yad. Fiz. 15 (1972) 781, Sov. J. Null. Phys. 15 (1972) 438; G. Albarelli, G. Parisi, Null. Phys. B 126 (1977) 298; Y.L. Downshifter, Sov. Phys. JETP 46 (1977) 641, Zhu. Esp. Toer. Fiz. 73 (1977) 1216. [17] J.A.M. Vermaelen, math-ph./0010025.

[18] F.W. Brasse, et al., Null. Phys. B 39 (1972) 421.

[19] A. Mucked, R. Engel, J.P. Rachen, R.J. Protheroe, T. Stanev, Compute. Phys. Common. 124 (2000) 290, atrophy/9903478.

[20] R.C. Walker, et al., Phys. Rev. D 49 (1994) 5671.